

Accepted Manuscript

Chang, J., Yang, G., Liu, S., Jin, H., Wu, Z., Xu, R., Min, Y., Zheng, K., Xu, B., Luo, W., Mao, F., Ge, Y. and Cheong, K.H. (2022), A Gradient Model for the Spatial Patterns of Cities. Adv. Theory Simul. 2100486. <https://doi.org/10.1002/adts.202100486>

A gradient model for the spatial patterns of cities

Jie Chang¹⁺, Guofu Yang^{1,2+}, Shun Liu¹, Hanhui Jin³, Zhaoping Wu¹, Ronghua Xu¹, Yong Min⁴, Kaiwen Zheng¹, Bin Xu⁵, Weidong Luo⁶, Feng Mao⁷, Ying Ge^{1*}, Kang Hao Cheong^{8,9*}

¹ College of Life Sciences, Zhejiang University, Hangzhou 310058, China

²Artistic Design & Creation School, Zhejiang University City College, Hangzhou 310015, China

³ School of Aeronautics and Astronautics, Zhejiang University, Hangzhou 310058, China

⁴ College of Computer Science and Technology, Zhejiang University of Technology, Hangzhou 310014, China

⁵ School of Public Administration, Zhejiang Gongshang University, 18 Xuezheng Street, Hangzhou, 310018, China

⁶ College of economics, Zhejiang University, Hangzhou 310058, China

⁷ School of Earth and Ocean Sciences, Cardiff University, Cardiff, CF10 3AT, United Kingdom

⁸ Science, Mathematics and Technology Cluster, Singapore University of Technology and Design (SUTD), 8 Somapah Road, S487372, Singapore

⁹ SUTD–Massachusetts Institute of Technology International Design Centre, Singapore

***Joint Corresponding authors: Kang Hao Cheong and Ying Ge**

E-mail: kanghao_cheong@sutd.edu.sg, geying@zju.edu.cn

†These authors contributed equally to this work.

1 **Abstract**

2 The dynamics of city's structures are determined by the coupling of functional
3 components (such as restaurants) and human population. Yet, there still lacks mechanism
4 models to quantify the forces on spatial distribution of the components. Here, a gradient
5 model is explored to simulate the individual density curves of multiple types of city
6 functional components based on the equilibria of gravitational and repulsive forces along
7 the urban-rural gradient. The model is concise for it relying four key variables, the
8 attributes of components include net ecosystem service (m) and environmental index (γ),
9 and the attributes of cities include land rent exponent (σ) and population attenuation
10 coefficient (β). The model has been used to simulate the distribution curves of 22 types of
11 components on the urban-rural gradients in 13 cities in two periods. The model reveals a
12 bottom-up mechanism that the patterns of the components in a city are determined by the
13 economic, ecological, and social attributes of both cities and components. Strongly
14 backed by empirical data, our model can predict the distribution curves of many types of
15 components along with the development of cities. This model provides a general tool for
16 analyzing the distribution of multiple objects on the gradients.

17

18 **Keywords:** environmental index, population pattern, urban-rural gradient, land rent,
19 transport costs.

20

1 **Main Text**

2 **Introduction**

3 A fascinating event in human activities is the formation, development, expansion,
4 and renewal of cities (1-3). A city is composed of human beings and multiple types of
5 functional components (or namely facilities), which are enterprises, firms, and other
6 institutions that provide goods and services for people (4, 5). The enclosed industrial
7 components are just defined as organaras (big organs) considering a modern industrial
8 city as a super-cell living system and a city center is a citynucleus (6). Some types of
9 components, such as banks and restaurants, are concentrated near citynucleus (7). In
10 contrast, as a city develops, some components, such as manufactories, tend to move
11 outward from the city center (8, 9), while some emerging industries (such as delivery
12 stores) spring up in the urban area (Fig. 1a). The emergence, coexistence, competition,
13 migration, and extinction of the components shape the spatial structure of the city (9-11).
14 The studies on city structure are limit in theoretical derivation and left many crucial
15 questions. For example, how much is the impact of land rent on the distribution of
16 functional components? How the population pattern drives the change of component
17 spatial distribution? How the residents' ecological preferences drive the change of
18 component distribution? To uncover the evolutionary mechanism of the components on
19 the gradients can deepen the fundamentally understood of city's functional spatial
20 structure.

21 In general, each type of functional component has many individuals in a city (5, 12,
22 13). For example, a type of fast food restaurant can be seen as a group and occupies a
23 niche in a city, a phenomenon akin to a biological population within a community (14).

1 The present models for the number of components are statistical and they study the
2 response of the local individual density of components—for example, the number of
3 restaurants, schools, hospitals, and banks—to the human population density in a location
4 (15-17). These models can explain neither the whole city’s structure nor the complex
5 driving forces—apart from the population—behind the distribution of components. A
6 series of spatial economic models, pioneered by von Thünen, can explain the mechanism
7 for the locations of land use types and functional components that affected by land rent
8 and transport cost gradients (3, 18, 19-21). However, these spatial economic models have
9 not involved the impact of people’s ecological preferences. This study adopts the physics
10 methodology while referring to the relevant theories of geography and tries to uncover
11 the mechanism of city structure and the evolution.

12

13 **The spatial pattern of city components in urban-rural landscapes**

14 In this paper, a ‘city’ means an urban-rural system, which has been defined as a
15 eukarcity (6). A great number of various types of functional components separate or
16 overlapping distribute in city core (citynucleus) and the periphery rural areas (Fig. 1a).
17 We investigate 24 types of components and choose 4 types that implement urban
18 processes that meet the living demands of the local residents. The real-world data of two
19 years of the components are investigated and compiled. Results showed that the
20 Kentucky Fried Chicken shops (KFC) are concentrated near the citynucleus (Fig. 1b), the
21 Zhongtong express outlets (ZTO), which provides domestic parcel service, are
22 concentrated on the outer side of KFCs; the cultivated greenhouses (GHs) are located in
23 suburban areas near the urban fringe, and the dairy farms (DF) are located in ex-urban

1 areas. Each type of component has $\sim 10^2$ to $\sim 10^3$ individuals in a city except for dairy
2 farms, which are rare (*SI Appendix, Table S1*). The individual density of a type of
3 component varied with the distance (d) from the city nucleus (*Fig. 1c*). The univariate
4 polynomial regressions show that, for a type of component, the individual density curve
5 has a peak (P_{max}), which is located at a position (d^*) along the urban-rural gradient (*Fig.*
6 *1c and SI Appendix, Table S2*). The rank correlation showed that the d^* of a type of
7 component is related to the supply ability of the target services, which is the economic
8 return to the investor for constructing and operating the components (*Fig. 1c, d*). An
9 exception is that the d^* of DF is outside GH although the net service, which is the sum of
10 target and accompanied services, of DF is higher than GH. We find that the higher γ
11 value, which is the ratio of environmental impacts to target services, pushes DF outside
12 GH (*SI Appendix, Table S2*), and we denote γ as the ‘environmental index’. The statistical
13 model (22) we used can help us acquire the characteristics of component distribution (*SI*
14 *Appendix, Table S2*), but cannot uncover the driving factors and mechanisms.

15

16 **Modeling overview**

17 The distribution patterns of the functional components are mainly driven by
18 economic factors (19, 23). The components, which are artificial systems, need to provide
19 enough economic returns (target services) to the investors. The economic constraints for
20 the distribution of components are the land rent and transport costs (23), while the
21 ecological constraints are environmental impacts (8). In an ideal city with no
22 geographical difference (19) and only one city nucleus, the human population density
23 monotonically decreases from the urban center to rural areas, within which the

1 components are located and provide services for people (Fig. 2a). The two-dimensional
2 pattern of attributes of city and components can be described as a one-dimensional
3 individual density curve along the urban-rural gradient, $P(d)$, in a city (Fig. 2b, c). It is
4 emphasized that, although the above principle depicts a single-center city, it also suitable
5 for polycentric cities. The gradient and equilibrium of gravitational and repulsive forces
6 can also be separated from the sub-center of a polycentric city.

7 The gravitational force (F_g) along an urban-rural gradient for a type of component is
8 mainly determined by the spatial pattern of the product's transport cost. For the life-
9 support components (such as restaurants), the cost of the products of a component is
10 negatively correlated to the density of local human population (Fig. 2d). The
11 transportation cost depends on human population density, road condition, and product
12 transportability (19, 24). Densely populated areas attract the distribution of functional
13 components (15, 25) due to a small average transportation distance (\bar{r}) from products to
14 consumers (SI Appendix, Fig. S9a). In the citynucleus, the population is much higher than
15 in urban fringe and rural areas (19, 24). For the human population density in locations in
16 response to the distance (d) from citynucleus, the exponent function ($Y = ae^{bX}$) is best fit
17 that support Clark (26) if the range limit to urban areas; while if include the suburban
18 area, the power law function is the best fit regressions (SI Appendix, Table S8),

$$19 \quad \text{Pop}(d) = Ad^\beta \quad (1)$$

20 where $\text{Pop}(d)$ is the average human population density of the ring located at distance d
21 from the citynucleus. The $\text{Pop}(d)$ values were measured through random quadrat
22 investigation on the ring (Fig. 2a). A is the fitted coefficient. The attenuation coefficient
23 (β) is for the human population density on the urban-rural gradient.

1 Based on the negative correlation between product transportation distance and
2 population density (23), the mean distance \bar{r} for a type of component at d ring is,

$$3 \quad \bar{r}(d) = -\beta \ln(d) \quad (2)$$

4 where $\bar{r}(d)$ is the average ‘last kilometer’ distance between the components’ products
5 and the consumers at location d on the urban-rural gradient, d and β are come from
6 equation (1).

7 The transport cost also depends on product transportability, which varied greatly
8 among different types of components. For example, we have found that the transport of
9 KFC’s take-out products is limited to 3 km in the case cities according to the distribution
10 rules of stores. With the development of the urban and peri-urban agriculture, the
11 vegetables from the greenhouse can be transported more than 30 km and keep fresh for
12 local acceptance (*SI Appendix, Fig. S9b*). The ‘iceberg transport model’ to calculate the
13 value loss in the transportation process (27) is introduced to calculate transport cost (C_T)
14 of the products,

$$15 \quad C_T(d) = I (1 - e^{-\tau \bar{r}}) \quad (3)$$

16 where $C_T(d)$ is the transport cost at location d on the urban-rural gradient, I is the
17 coefficient for the initial value of a type of product; $\tau \in (0,1)$ is the iceberg coefficient,
18 which is the proportion of value lost per unit of distance transported.

19 Combining equations (2) and (3),

$$20 \quad F_g(d) = I(1 - e^{\tau \beta \ln(d)}) = I(1 - d^{\tau \beta}) \quad (4)$$

21 where $F_g(d)$ is the gravitational force on urban-rural gradient in a city. Equation (4)
22 shows that the attraction is monotonic decreasing from citynucleus to rural area (*Fig. 2d*).

1 The repulsive force (F_r) along an urban-rural gradient is monotonic decreasing from
2 citynucleus outward. Generally, the high land rent (LR) repulses some low economic
3 output components away from the city center (19, 28). Only the components with high
4 economic output can be located near the citynucleus as they can afford paying the high
5 land rent. We have found that the land rents (LR) in most cities were power law
6 decreasing on the urban-rural gradient (18),

$$7 \quad LR(d) = cd^\sigma \quad (5)$$

8 where $LR(d)$ is the land rents at location d on the urban-rural gradient, c is the land rent
9 coefficient (USD m⁻² yr⁻¹), and σ is the land rent attenuation coefficient.

10 Besides the impact of land rent, a functional component's economic outputs (m) and
11 people's preference for environmental impacts also affect the F_r for a type of component,
12 i.e.,

$$13 \quad F_r(d) = LR(d) / (m/\gamma) = cd^\sigma / (m/\gamma) \quad (6)$$

14 where $F_r(d)$ is the repulsive force at location d on the urban-rural gradient, γ is the
15 absolute value, $m > 0$. Equation (6) means that a larger net ecosystem service enables a
16 component to be distributed near the citynucleus, while a larger ecosystem dis-service
17 pushes the component outwards (*SI Appendix, Fig. S9c*). For example, with the social
18 prosperity in recent decades, the components with high environment impacts are moved
19 far from the citynucleus due to people's growing preference for better environmental
20 quality.

21 The minimum of gravitational plus repulsive forces ($F_g + F_r$), E , is changing with
22 the development of city, and it is also different among different types of components in a
23 city (*Fig. 2d*). The optimum location (d^*) corresponds to the E for a type of component

1 on the urban-rural gradient where the maximum individual density (P_{max}) occurs (Fig. 2b,
2 c). Each type of component has a d^* and some of them can overlap due to fact that they
3 are distributed across different locations within a ring (Fig. 2a).

4 The total amount of a type of component and the P_{max} in a city is determined by the
5 total demand (M) and the net ecosystem service (m) of the component. We follow the
6 form of Newton's gravity model and take the product of these two terms ($M \times m$) as the
7 numerator term. Then the individual density of a type of component along an urban-rural
8 gradient is

$$9 \quad P(d) = G \frac{M \times m}{Fg(d) + Fr(d)} \quad (7)$$

10 where $P(d)$ is the component density t location d on the urban-rural gradient, G is a
11 coefficient to adjust the order of magnitude of the $M \times m$ multiplier.

12 When equations (4) and (6) are substituted into equation (7), we get that the
13 individual density curve of a type of component on the urban-rural gradient is

$$14 \quad P(d) = G \frac{M \times m}{l(1 - d^{\alpha\beta}) + cd^{\sigma}/(\frac{m}{\gamma})} \quad (8)$$

15 The constant of proportionality (G) in equation (8) will be acquired via the
16 simulation of the real-world data.

17

18 **Model optimization**

19 The input variables were calculated using the above equations and then simulate the
20 individual density curves using equation (8). The model fitting is based on the
21 Levenberg-Marquardt algorithm, which can provide numerical solutions of nonlinear
22 minimization (local minimum). The parameters and coefficients (SI Appendix, Table S3,

1 [Tables S5,6,9](#)) were input to the nonlinear fitting module (using Origin Pro 2018,
 2 OriginLab Corporation) to estimate the coefficients (G, I) by fitting the real-world data of
 3 the 4 types of functional components in 13 cities. The fitting accuracy of the model
 4 parameters is evaluated and improved in iteration and this process continues until the
 5 accuracy of the model parameters can no longer be improved. Unfortunately, the
 6 simulated distribution individual density curves of KFC, ZTO and GH on the urban-rural
 7 gradient in most cities were not good fits to the data, and particularly, the kurtosis did not
 8 conform to the real-world data. This means that equation (8) overlooks some factors.

9 After re-evaluation, a new parameter, Z , was introduced into the denominator of the
 10 model. Finally, we finish the construction of a gradient model for functional components
 11 along urban-rural gradients,

$$12 \quad P(d) = G \frac{M \times m}{I(1 - d^{\tau\beta}) + cd^{\sigma}/(\frac{m}{\gamma}) + Z} \quad (9)$$

13 where parameter Z represents the other factors besides the gravitational and repulsive
 14 forces in the model and we dubbed Z as the ‘city index’ due to it being related to the city
 15 attributes revealed by statistics. We did not further simplify the mathematical form of
 16 equation (9) because each parameter has physical significance and corresponds to the
 17 mechanism behind the distribution of components.

18 All the meanings of the model parameters are shown in [Table 1](#). After validating the
 19 simulation of distribution of multiple types of components, the gradient model (eq 9) was
 20 used to predict the patterns of components in different periods or different cities.

21

22 **Table 1.** The parameters and their significance in the gradient model

Parameters	Symbol
Input variable	
Total demand for specific goods and services of cities	M
Net ecosystem services of the components	m
Iceberg attenuation index in transportation of products	τ
Coefficient of statistical function of population distribution	β
Distance from citynucleus	d
Coefficient of statistical function of land rent distribution	c
Land rent attenuation power	σ
Ratio of ecosystem dis-services to target services	γ
Simulated or adjusted parameter	
Adjustment constant for $M \times m$	G
Coefficient in transport cost function	I
City index	Z

1

2 **Results**

3 **Model simulation and validation**

4 Using the model (eq 9), we run the fitting module again. The simulated individual
5 density curves coincide with the real-world data in two periods (Fig. 3a-d and *SI*
6 *Appendix, Table S3*). Results showed that the fittings are significant (the minimum $R^2 >$
7 0.72 of the fitting curves). The individual density curves and the relationships between
8 the gravitational and repulsive forces support our hypothesis in Fig. 2. The simulation for
9 the individual density curves of the components shows that the repulsive forces to the
10 four components are ordered $KFC < ZTO < GH < DF$, and so are the gravitational forces
11 (Fig. 3e-h). The minimum points (E) of repulsive plus gravitational forces correspond to
12 the d^* (*SI Appendix, Table S2*). For example, along with the development of Shanghai

1 City, the curve of land price and population along the urban-rural gradients tend to be
2 gentle (absolute values of σ and β decrease), resulting in the P_{max} of KFC, ZTO, GH and
3 DF decreasing by 20%, 29%, 13%, and 21% respectively, and all the d^* moving outwards
4 (Fig. 3a-d). The reason is that with the development of the city, both gravitational and
5 repulsive forces for the four components increase and the equilibrium changes (Fig. 3e-
6 h). All the above model behaviors support our hypothesis in Fig. 2, which is that the
7 equilibrium of forces determines the d^* , and the city's attributes determine P_{max} . In
8 addition, the d^* of GH is located at the edge of the built-up area, which reflects the shape
9 and size of the urban area (Fig. 3c). This means that the driving force of the components
10 quantified by the gradient model can be used to study the evolution of the scale of cities.

11 The 4 types of components simulated by the gradient model in 13 cities showed that
12 all the individual density curves of the components fitted the real-world data significantly
13 except for KFC in Shaoxing City and ZTO in Jiaxing City, where there are insufficient
14 individuals for simulation (Fig. 3-4 and *SI Appendix*, Fig. S1). The individual density
15 curves of KFC, ZTO, GH and DF were simulated well by gradient ($P < 0.05$), with
16 average R^2 of 0.88, 0.81, 0.77, and 0.87, respectively. More importantly, the gradient
17 model can simulate the individual density curves of multiple components (based on
18 corresponding coefficients and parameters) in a city at the same time, and simulate their
19 coexistence at any location within cities (Fig. 4 and *SI Appendix*, Fig. S2). The gradient
20 model clearly shows the mechanism of gravitational-repulsive force shapes the specific
21 niche of components on the urban-rural gradient (*SI Appendix*, Fig. S3).

22

23 **Prediction and application ability of the gradient model**

1 In order to validate the robustness and the predictive power of the gradient model,
 2 we analyze the relationships between the coefficients of the model and the attributes of
 3 the case cities and components. Regression analysis shows that the Z of the components
 4 which are located in urban areas are related to urban central land price (c), while the Z of
 5 components which are located in rural areas are most closely related to urban areas (*SI*
 6 *Appendix, Fig. S4*). However, I is not related to any attributes. We then try to find if there
 7 are indirect relationships, and then the aggregate force of the model, the gravitational and
 8 repulsive forces is derived,

$$9 \quad F'(d^*) = \left[I(1 - d^{*\tau\beta}) + cd^{*\sigma} / \left(\frac{m}{\gamma}\right) \right]' = 0 \quad (10)$$

10 where the symbols are the same as in equation (9). When the sum of gravitational and
 11 repulsive forces is the minimum, the individual density of components reaches the peak
 12 value, and the derivative of the sum of repulsive and gravitational forces is 0. Therefore, I
 13 can be calculated via

$$14 \quad I = \frac{c\gamma\sigma}{\tau\beta m} d^{*\sigma-\tau\beta} \quad (11)$$

15 The G value of the same type of component can be obtained by the geometric mean
 16 of the same component in multiple cities,

$$17 \quad G = \left(\prod_{i=1}^N G_i \right)^{1/N} \quad (12)$$

18 where G_i is the constant of proportionality in city i , the value of which is obtained by
 19 model fitting, and N is the number of the case cities.

20 The regression analysis showed that the d^* of a type of component was significantly
 21 related to the urban population of the 13 cities (*SI Appendix, Fig. S4*). Then I can be
 22 derived from d^* , which is determined by the gravitational and repulsive force. In order to

1 study the effects of city development on component distribution, the attributes of the
2 latest period in Hangzhou and Ningbo were used to predict the distribution of KFC, ZTO
3 and GH over time. The predictions matched the 3 components' distribution curves well
4 ($R^2 > 0.53$, *SI Appendix, Fig. S5*).

5 The magnitudes of the average G of KFC and ZTO located in urban areas are both
6 10^{-12} , while the magnitudes of the average G of GH and DF located outside the city are
7 10^{-6} and 10^{-8} respectively. The difference in the G values of components inside and
8 outside the city is of 4-6 orders of magnitude (*SI Appendix, Table S4*).

9 We predict the individual density curves of the four types of components in the other
10 two cities (Wuhan and Nanjing City) according to the relationships between the model
11 parameters and the attributes in 13 cities (*SI Appendix, Fig. S4*). The predicted curves
12 match well ($P < 0.05$) with the real-world data of the distribution of components
13 (respectively, *SI Appendix, Fig. S6*). The predictions validate the universality of the
14 model among different cities (*SI Appendix, Tables S5-6*). Furthermore, the gradient model
15 could be extend to simulates many types of components co-exist in an urban-rural system
16 (*SI Appendix, Fig. S7*).

17

18 **Discussion**

19 John von Neumann used to say, “with four parameters I can fit an elephant” (29). It
20 means that excessive arbitrary parameters made model loss the significance. Fortunately,
21 our gradient model has only one arbitrary parameter G , and the other two parameters I
22 and Z , can be calculated from real-world data (*SI Appendix, Fig. S4*). The parameters
23 used in the gradient model are easy to observe and calculated, and the simulation results

1 can be verified by filed investigations. It means that our gradient model is reliable and
2 robust, for it stands on the solid ground of physics. Former models mainly consider the
3 two-dimensions mainly identify ‘islands’ or ‘lowlands’ in urban area for some parameters
4 (9). Their data and analysis can easily be transformed and apply this 1-Dimensional
5 gradient model and quantify the relevant variables of spatial distribution of components,
6 including the economic revenue, population distribution and ecological preference. For
7 example, this 1-dimensional gradient model can provide a quantitative demonstration to
8 Christaller's central hypothesis (30). Urban planners can use this model to accurately
9 predict how cities will develop over time, by consider the changes of population, land
10 rent and ecological consciousness.

11 The sensitivity analysis of the gradient model shows that the distributions of
12 multiple types of components are more sensitive to four input parameters, m , γ , σ and r ;
13 than other parameters. These four parameters largely determine the gravity and repulsion
14 forces (*SI Appendix, Table S7*). It means that the attributes of components together with
15 the attributes of cities jointly determine the functional spatial structure of cities. The
16 attributes of components include net ecosystem service (m) and environmental index (γ),
17 and the attributes of cities include land rent exponent (σ) and population attenuation
18 coefficient (β). Many researchers find that the land rent and freight rate affect the
19 distribution of components (21), but few models quantify the affections. This 1-
20 dimensional gradient model quantifies the influence of driving factors and find out the key
21 factors. For example, the ecosystem service intensity m of greenhouses is much smaller
22 than that of KFCs, so it cannot afford the high land rent, therefore they are repulsed by
23 the city center. Meanwhile, the fresh-keeping distance r of greenhouse products is longer

1 than that of KFCs, so they are less attracted by the city center. The equilibrium of the two
2 forces mainly drives those greenhouses locate outside urban areas and far from other
3 functional components.

4 The gradient model uncovers the social-economic and ecological mechanism of
5 development of city's functional structure. The technological innovations of the
6 components increase the productivity m while decreasing the environmental impact γ of
7 the components. The improvements of the net benefit (combined m and γ) of the
8 components raise the gravitation force to the components and then uplift the individual
9 density peak (P_{max}) of the individuals and pull the P_{max} to move inward (d^* decreases) on
10 urban-rural gradients. (*SI Appendix, Fig. S8*). These results support the view that the
11 enterprises (city functional components or organaras) have to keep up with technological
12 innovations continuously (12, 31). Furthermore, the individual density curve response of
13 to the environmental index γ reveals that innovations must also reduce the environmental
14 impact of components in order to adapt to the changes in human preference, which tends
15 to be stricter on environment quality with increasing social prosperity (32, 33). The
16 super-cell city model has analyzed the spatial relationships between organaras and
17 citynucleus (6). The gradient model further quantifies the important impacts of the
18 production capacity, ecological characteristics, and technological progress of organaras
19 on the city's functional spatial structure.

20 The land rent reflects the result of competition among components for a scarce land
21 resource (28). The development of cities flattens the spatial patterns of land rent and
22 human population (18). As the land rent curves become gentler, the P_{max} of the four types
23 of components decrease, but only the d^* of GH and DF located outside the urban area

1 moves outward (*SI Appendix, Table S7*). In other words, the growth of population in the
2 peripheries of the city is caused by the urbanization (*SI Appendix, Fig. S9b*) will stimulate
3 the P_{max} of components move outward (*SI Appendix, Fig. S8*). The dynamics of cities,
4 which include urbanization, counter urbanization, and re-urbanization, are essentially the
5 change of the city attributes (13). For example, the changes in economic level, population
6 size, urban area and structure (3, 9, 34). The change in total demand for the goods or
7 services of a type of component in a city (M) reflects the dynamics of the population and
8 its preferences, and it affects the P_{max} . The city index Z , which is highly related to the
9 maximum land rent and the size of the city's urban area (*SI Appendix, Fig. S4*), enhances
10 the P_{max} but maintains the position of d^* (*SI Appendix, Fig. S8*). Through above
11 mechanism, the gradient model could help us to quantify the self-organization processes
12 of a eukarcity, including coexistence of and competition between different types of
13 organaras revealed by Chang et al. 2021 (6). The mechanism could be the basis for
14 predicting the future city structure based on the city's attributes along with the
15 development of cities.

16 Although each case city has its unique spatial structure and development trend, the
17 gradient model in this study has been proven the generality to analyze the spatial
18 distribution of city functional components. Actually, the key input parameters are the
19 spatial distribution function of human population and land price and the component
20 production capacity. We consider that the model has the potential to apply in other cities
21 around the world. On the one hand, we have found the trends of land rent curve and
22 population density curve along the urban-rural gradient of some cities in the United
23 States, Japan, South Korea, Australia and Europe are similar to the patterns of the Chines

1 cities, and it shows the monotonic attenuation trend from city center outward (18,35). On
2 the other hand, recent studies have shown that the affluent population mainly occupies
3 the position of urban center, even in mega cities such as New York and London (36) that
4 similar to the case Chinese cities in this study. Although some rich people tend to live in
5 the outer suburbs, the small population cannot change the spatial pattern of high
6 accessibility of urban center. Therefore, once the input parameters were obtained, the
7 model could be used to describe the distribution pattern of functional components in
8 other cities worldwide. In the future, the studies can be carried out across regions and
9 countries for comparing the similarities and differences of diverse cities and countries,
10 and reveal the principle behind the phenomenon.

11 This model integrates the various factors and their interactions into a one-dimensional
12 urban-rural gradient and finds quantified rules. This static model describes the interaction
13 results of various factors as the eco-economic system in relative equilibrium state. Such a
14 mechanism model, instead of the statistic model (7), reveals the general law of the
15 development, expansion, and renewal of the cities. This mathematical gradient model
16 deepens the understanding of city structure based on a conceptual super cell model (6).
17 Based on the historical distributions of the functional components and related parameters,
18 the model can be used to predict the development the city morphology and structure. The
19 model can also help to explore the limitations of the current city in structure and function,
20 and to find out the crucial optimization points to promote sustainable development in the
21 context of global urbanization. It can be further developed and inspire interdisciplinary
22 studies across fields such as ecology, economics, urban planning and management, and
23 engineering.

1

2 **Materials and Methods**

3 **Selection of case cities and functional components**

4 The criteria for choosing case cities: (1) the data for the population and spatial
5 pattern of population of the city is available; (2) the data for the spatial pattern of land
6 price of the city is available; (3) a city is self-sustainable with complete processes and
7 function. According to the criteria, we selected 15 cities in China: Shanghai, Beijing,
8 Tianjin, Suzhou, Wuhan, Hangzhou, Nanjing, Wuxi, Ningbo, Nantong, Hefei,
9 Changzhou, Shaoxing, Jiaxing, and Zhenjiang City, and several time periods in some
10 cities (*SI Appendix, Table S1*). The criteria for choosing the type of component: (1) the
11 function of the components is to provide services to people locally, so their amount is
12 related to the population of the city; (2) each component has a number of individuals that
13 form an individual density distribution curve along the urban-rural gradient; (3) different
14 types of components have distinguishable distribution curves along the urban-rural
15 gradient: one type is concentrated near the citynucleus, one type outside the center, one
16 type is near the urban fringe, and one is in the ex-urban area. According to the criteria, we
17 chose: (1) a type of fast food restaurant, Kentucky Fried Chicken shop (KFC), most of
18 which are near the citynucleus; (2) a type of express delivery outlets, ZTO delivery
19 outlets, most of which are outside the citynucleus, (3) a primary biological production
20 component, cultivated greenhouses, which are mainly outside but near the suburban area,
21 (4) a type of secondary biological production component, dairy farms, that are mainly
22 located in ex-urban areas (*SI Appendix, Fig. S10*).

23

1 **Data source and ecosystem services assessment**

2 The data of city attributes and functional components are obtained by investigation
3 or public database, the details see Supplementary Information. Through the surveying and
4 mapping of the land price of cities, it is found that there are still a large number of single-
5 center cities. Of course, the research on multi-center cities may be disturbed, and needs
6 further study. According to the Millennium Ecosystem Assessment, ecosystem services
7 include provisioning services, regulating services, cultural services, and supporting
8 services (37). In this study, the ecosystem services (goods and services) provided by
9 artificial ecosystems (components) are divided into target services and accompanied
10 services separately (*SI Appendix, Fig. S11*) (7). The calculations of the ecosystem
11 services of the components see Supplementary Information.

12 The target services of a type of component are determined by the investment goal of
13 the artificial ecosystem. This means that they can be the provisioning, regulating, or
14 cultural services in Millennium Ecosystem Assessment (37). The target service of KFC,
15 greenhouses, and dairy farms is the provisioning of food, which is equivalent to some of
16 the provisioning services of natural ecosystems, while the target service of ZTO is the
17 regulating service of distributing goods to people. The accompanied services are
18 equivalent to the externalities (positive or negative) in economics. They can be
19 categorized into provisioning, regulating or cultural services. Regulating services are
20 further divided into positive (services) and negative (dis-services) in this paper, following
21 the guidelines in Liu et al. (38).

22 The net service (NES, m in model) is the sum of the ecosystem services (target
23 service + positive regulating services + cultural services) and dis-services (environmental

1 impacts),

$$2 \quad \quad \quad NES = \sum_{i=1}^n ES_i \quad (13)$$

3 where ES_i (USD m⁻² yr⁻¹) is the value of ecosystem service i , and n is the number of
4 ecosystem services considered in this study.

5 Environmental index (γ in model) is calculated by the ratio of target goods and
6 services (TGS) to dis-services (EDS) of a type of component,

$$7 \quad \quad \quad \gamma = |EDS| / TGS \quad (14)$$

8

9 **Statistics**

10 The statistic functions for the attributes of cities and components with distance from
11 the citynucleus uses linear and nonlinear regressions (Excel 2019, Microsoft
12 Cooperation). Linear and nonlinear regressions were used to study the relationship
13 between Z and the city attributes, and the best adjusted R^2 was used to select the
14 regression form.

15 The nonlinear fitting module in Origin 2018 Pro (OriginLab Corporation) was used
16 to simulate the spatial distribution of functional components. As the initial values of
17 nonlinear fitting parameters may affect the simulation results, we carefully cycle through
18 the appropriate initial values. At the beginning of the model iterative process, we use the
19 default value of 1 as the initial value for G and I . Meanwhile, we fix Z as 0, because Z
20 only affects the P_{max} without the peak position. After the model iteration is over at this
21 stage, we relax the condition on Z and continue with the iterative process to obtain the
22 final fitting parameters.

1 **Acknowledgments**

2 This work was financially supported by the National Natural Science Foundation of
3 China (Grant No. 31870307). We thank Qu Z., Pan K., Zhu K, Shi M. Wong Y., Guo K.,
4 Zhang T. for the contributions.

5

6 **Author Contributions:** J.C. and Y.G. designed the study; G.Y., S.L., F.M., Y.M. and
7 K.Z. developed the model; H.J., Z.W. and R.X. performed data collection; H.J., Z.W. and
8 R.X., K.H.C. analyzed the data; B.X., W.L. undertook the economic analysis; J.C., Y.G.,
9 G.Y. and K.H.C. wrote the manuscript. All authors performed research and approved the
10 manuscript.

11

12 **Competing Interest Statement:** The authors declare no competing interests.

13

1 **References**

- 2 1. D. Helbing, J. Keltsch, P. Molnár, Modelling the evolution of human trail systems.
3 *Nature* **388**, 47–50 (1997).
- 4 2. M. Batty, The Size, Scale, and Shape of Cities. *Science* **319**, 769–771 (2008).
- 5 3. L. M. A. Bettencourt, The Origins of Scaling in Cities. *Science* **340**, 1438–1441 (2013).
- 6 4. A. Ramaswami, A. G. Russell, P. J. Culligan, K. R. Sharma, E. Kumar, Meta-
7 principles for developing smart, sustainable, and healthy cities. *Science* **352**, 940–
8 943 (2016).
- 9 5. R. Xu, *et al.*, City components–area relationship and diversity pattern: towards a better
10 understanding of urban structure. *Sustainable Cities and Society* **60**, 102272 (2020).
- 11 6. J. Chang, *et al.*, Modern cities modelled as “super–cells” rather than multicellular
12 organisms: Implications for industry, goods and services. *BioEssays*, 2100041
13 (2021).
- 14 7. S. Liu, *et al.*, Studying the distribution patterns, dynamics and influencing factors of
15 city functional components by gradient analysis. *Scientific Reports*, **11**, 1–13 (2021).
- 16 8. B. Gao, W. Liu, D. Michael, State land policy, land markets and geographies of
17 manufacturing: The case of Beijing, China. *Land Use Policy* **36**, 1–12 (2014).
- 18 9. J. V. Henderson, A. J. Venables, T. Regan, I. Samsonov, Building functional cities.
19 *Science* **352**, 946–947 (2016).
- 20 10. M. Batty, Competition in the Built Environment: Scaling Laws for Cities,
21 Neighbourhoods and Buildings. *Nexus Netw J* **17**, 831–850 (2015).
- 22 11. L. Wu, C. Gong, X. Yan, Taylor’s power law and its decomposition in urban facilities.
23 *Royal Society Open Science* **6**, 180770 (2019).

- 1 12. G. B. West. *Scale: the universal laws of growth, innovation, sustainability, and the*
2 *pace of life in organisms, cities, economies, and companies.* (Penguin, 2017).
- 3 13. M. Barthelemy, The statistical physics of cities. *Nature Reviews Physics*, 1 (2019).
- 4 14. R. M. Pringle, *et al.*, Predator-induced collapse of niche structure and species
5 coexistence. *Nature* **570**, 58–64 (2019).
- 6 15. J. Um, S.-W. Son, S.-I. Lee, H. Jeong, B. J. Kim, Scaling laws between population
7 and facility densities. *PNAS* **106**, 14236–14240 (2009).
- 8 16. J. Gutiérrez, J. C. García-Palomares, G. Romanillos, M. H. Salas-Olmedo, The
9 eruption of Airbnb in tourist cities: Comparing spatial patterns of hotels and peer-to-
10 peer accommodation in Barcelona. *Tourism Management* **62**, 278–291 (2017).
- 11 17. Y. Yang, W. S. Roehl, J.-H. Huang, Understanding and projecting the restaurantscape:
12 The influence of neighborhood sociodemographic characteristics on restaurant
13 location. *International Journal of Hospitality Management* **67**, 33–45 (2017).
- 14 18. J. Chang, *et al.*, Assessing the ecosystem services provided by urban green spaces
15 along urban center-edge gradients. *Scientific Reports* **7** (2017).
- 16 19. W. Alonso. *Location and land use. Toward a general theory of land rent.* (Harvard
17 Univ Press, 1964).
- 18 20. D. J. Egan, K. Nield, Towards a Theory of Intraurban Hotel Location. *Urban Studies*
19 **37**, 611–621 (2000).
- 20 21. J. Gao, W. Chen, F. Yuan, Spatial restructuring and the logic of industrial land
21 redevelopment in urban China: I. Theoretical considerations. *Land Use Policy* **68**,
22 604–613 (2017).

- 1 22. J. Fan, *et al.*, Universal gap scaling in percolation. *Nature Physics* **16**, 455–461
2 (2020).
- 3 23. W. Chatti, B. Ben Soltane, T. Abalala, Impacts of Public Transport Policy on City
4 Size and Welfare. *Netw Spat Econ* **19**, 1097–1122 (2019).
- 5 24. D. J. Weiss, *et al.*, A global map of travel time to cities to assess inequalities in
6 accessibility in 2015. *Nature* **553**, 333–336 (2018).
- 7 25. G. Manoli, *et al.*, Magnitude of urban heat islands largely explained by climate and
8 population. *Nature* **573**, 55–60 (2019).
- 9 26. C. Clark. Urban population densities. *Journal of the Royal Statistical Society. Series A*
10 (General) **114**, 490–496 (1951).
- 11 27. P. McCann, Transport costs and new economic geography. *Journal of Economic*
12 *Geography* **5**, 305–318 (2005).
- 13 28. T. Sakai, K. Kawamura, T. Hyodo, Spatial reorganization of urban logistics system
14 and its impacts: Case of Tokyo. *Journal of Transport Geography* **60**, 110–118
15 (2017).
- 16 29. J. Lever, M. Krzywinski, N. Altman, Model selection and overfitting. *Nature*
17 *Methods* **13**, 703–704 (2016).
- 18 30. W. Christaller. *Central places in southern Germany*. (Prentice Hall, 1966).
- 19 31. L. M. A. Bettencourt, J. Lobo, D. Helbing, C. Kühnert, G. B. West, Growth,
20 innovation, scaling, and the pace of life in cities. *PNAS* **104**, 7301–7306 (2007).
- 21 32. D. E. Bloom, D. Canning, G. Fink, Urbanization and the Wealth of Nations. *Science*
22 **319**, 772–775 (2008).

- 1 33. G. S. Cumming, *et al.*, Implications of agricultural transitions and urbanization for
2 ecosystem services. *Nature* **515**, 50–57 (2014).
- 3 34. M. Batty, A Theory of City Size. *Science* **340**, 1418–1419 (2013).
- 4 35. M. Kulish, A. Richards, C. Gillitzer., Urban structure and housing prices: Some
5 evidence from Australian cities. *Economic Record*, **88**, 303-322 (2012).
- 6 36. M. van Ham, M. Uesugi, T. Tammaru, D. Manley, H. Janssen, Changing
7 occupational structures and residential segregation in New York, London and Tokyo.
8 *Nature Human Behaviour*, **4**, 1124-1134 (2020).
- 9 37. Millennium Ecosystem Assessment. *Ecosystems and Human Well-Being: Synthesis*
10 (Island Press, 2005).
- 11 38. D. Liu, *et al.*, Constructed wetlands as biofuel production systems. *Nature Clim.*
12 *Change* **2**, 190–194 (2012).
- 13 39. National Bureau of Statistics of China. *China city statistical yearbook 2020*. (China
14 Statistics Press, 2020).
- 15 40. Ministry of Housing and Urban-Rural Development of China. *China urban-rural*
16 *construction statistical yearbook 2020*. (China Statistics Press, 2020).
- 17 41. A. J. Tatem, WorldPop, open data for spatial demography. *Sci Data* **4**, 170004
18 (2017).
- 19 42. A. E. Gaughan, *et al.*, Spatiotemporal patterns of population in mainland China, 1990
20 to 2010. *Scientific Data* **3**, 160005 (2016).
- 21 43 J. Chang, *et al.*, Assessment of net ecosystem services of plastic greenhouse vegetable
22 cultivation in China. *Ecological Economics* **70**, 740–748 (2011).

- 1 44. X. Fan, *et al.*, Recoupling Industrial Dairy Feedlots and Industrial Farmlands
2 Mitigates the Environmental Impacts of Milk Production in China. *Environ. Sci.*
3 *Technol.* **52**, 3917–3925 (2018).
- 4 45. I. A. Curtis, Valuing ecosystem goods and services: a new approach using a surrogate
5 market and the combination of a multiple criteria analysis and a Delphi panel to
6 assign weights to the attributes. *Ecological Economics* **50**, 163–194 (2004).
- 7 46. Y. Wang, *et al.*, Quantification of net carbon flux from plastic greenhouse vegetable
8 cultivation: A full carbon cycle analysis. *Environmental Pollution* **159**, 1427–1434
9 (2011).
- 10 47. M. Goedkoop, *et al.*, ReCiPE 2008: A life cycle impact assessment method which
11 comprises harmonised category indicators at the midpoint and the endpoint level
12 (2008).
- 13
14

1 **Figures and Tables**

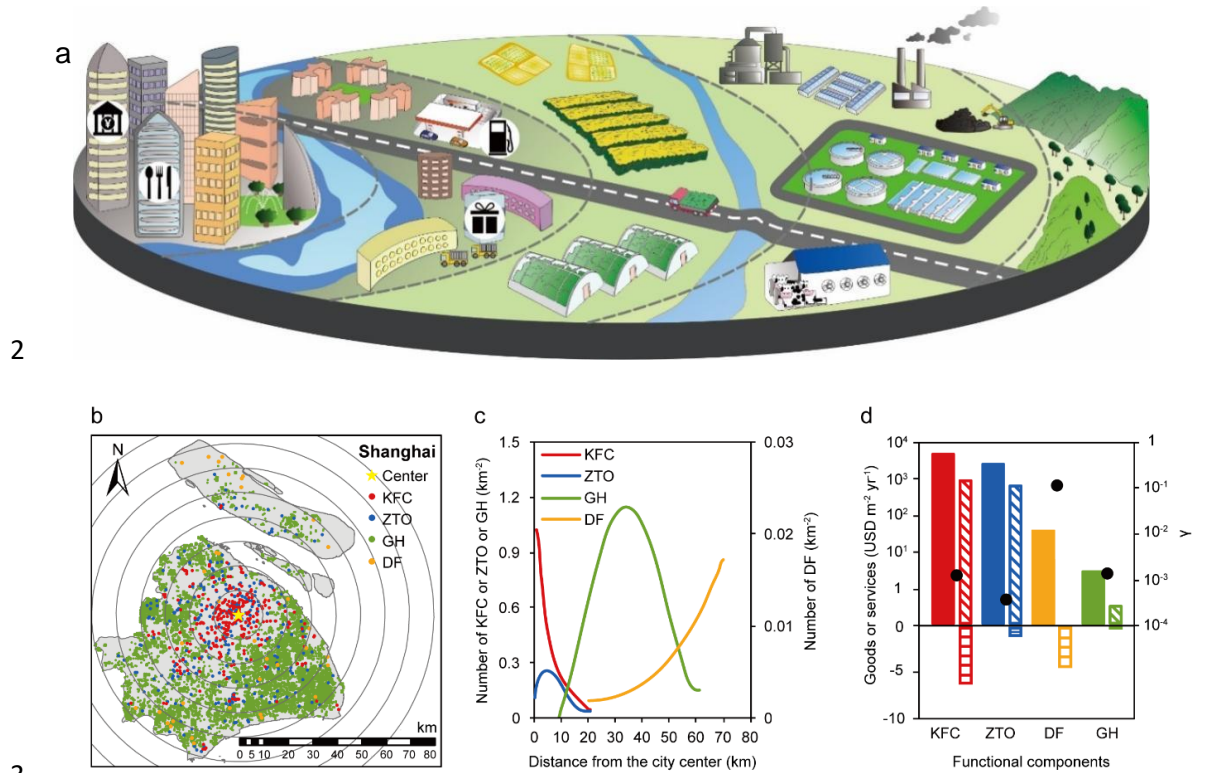
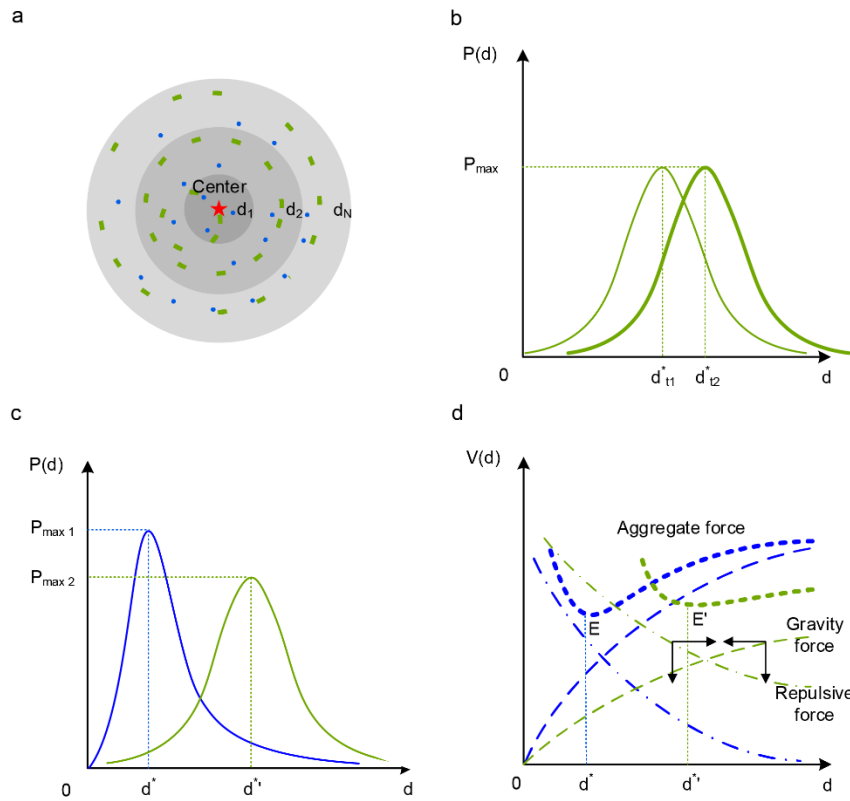


Figure 1. A city's layout indicated by functional components. **a**, Illustration of multiple types of components distributed from city nucleus to rural area; **b**, two-dimensional pattern of four types of components in Shanghai City, KFC—Kentucky Fried Chicken shops, ZTO—ZTO express outlets, GH—greenhouses, DF—dairy farms; **c**, one-dimensional individual density curves of the four types of components along the urban-rural gradient; **d**, ecosystem services of the four types of components, solid bar: target services, diagonal bar: accompanied services, horizontal bar: dis-services, black points: γ (absolute value of the ratio of dis-service/target services) of the components.



1

2 **Figure 2. Model hypothesis for the mechanism of the spatial distribution of city**

3 **components. a,** In an ideal city, the two-dimensional distribution patterns of population

4 and functional components obtain their highest individual density at the center and

5 become sparser farther out. The colors of the points indicate the different types of

6 components, and the colors of the ring from dark to gray indicate the human population

7 density from high to low; **b,** location of the individual density peak (P_{max}) of one type of

8 component shifts along the urban-rural gradient (d^*_{t1} to d^*_{t2}) with time; **c,** the distribution

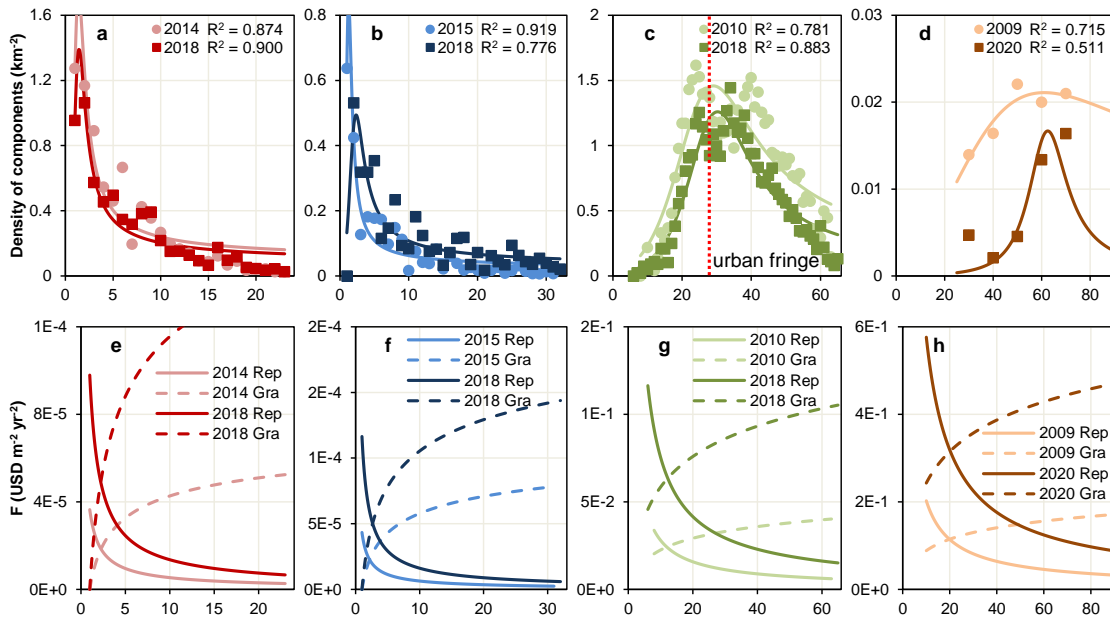
9 of two types of components along the urban-rural gradient. The d^* and $d^{*'}$ of P_{max}

10 correspond to the locations of E and E' in Fig. 2d, colors of lines correspond to the

11 types of components in Fig. 2d; **d,** repulsive force (dash-dotted line) and reverse gravity

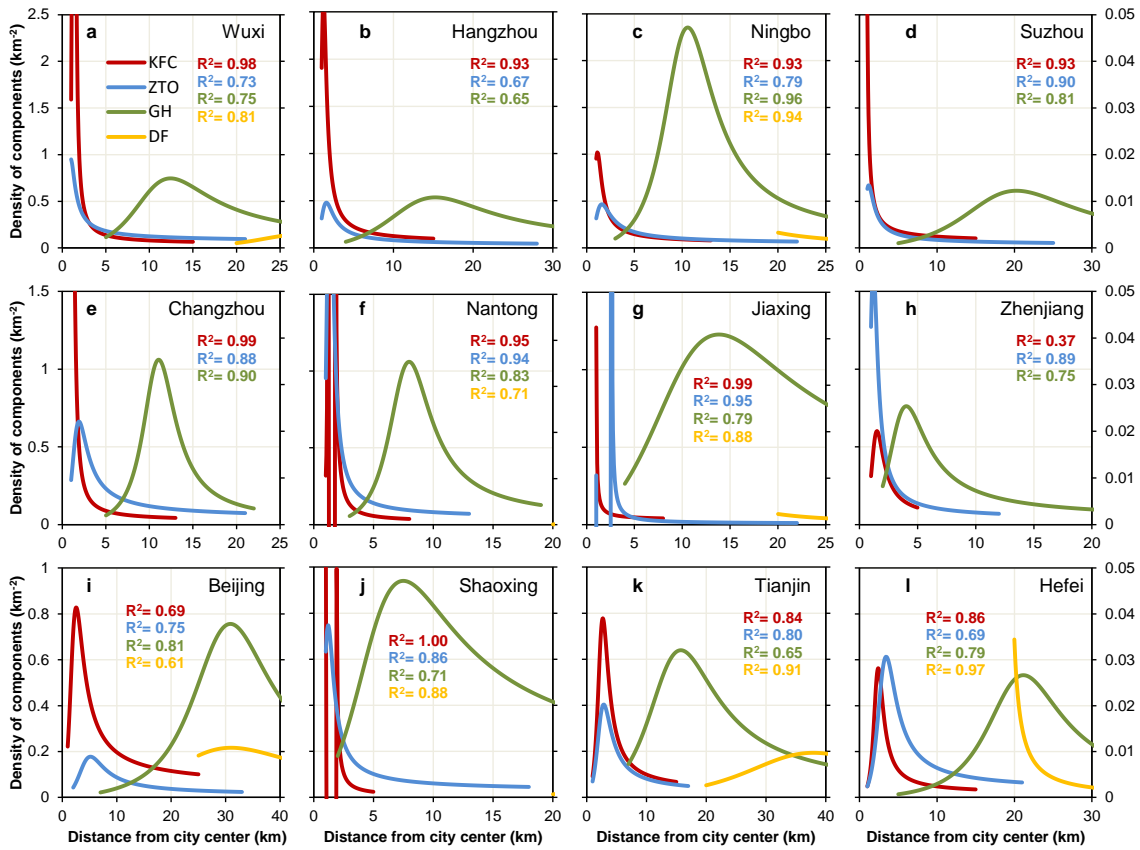
12 force (thin dashed line) for components on an urban-rural gradient, the thick dashed lines

- 1 show the aggregate forces, and the colors of the lines are corresponding to the types of
- 2 components in [Fig. 2a](#), E and E' are the minimum aggregate forces, and arrows indicate
- 3 the directions in which forces act on the components.
- 4



1
2
3
4
5
6
7
8
9

Figure 3. Simulated individual density curves of the components and the driven forces in Shanghai City in two periods. a-d, Simulated individual density curves and real-world data of the four types of components along the urban-rural gradient: **a,** Kentucky Fried Chicken shops; **b,** ZTO Express outlets; **c,** cultivated greenhouses, red dotted line indicates the location of the urban fringe; **d,** dairy farms; **e-h,** the repulsive force (solid line) and the reverse-gravitational force (dashed line) of the components correspond to a-d, respectively.



1

2

3 **Figure 4. Simulated spatial distribution of 4 types of components in 12 case cities.**

4 The individual density of Kentucky Fried Chicken shops (KFCs), ZTO Express outlets

5 and cultivated greenhouses (GHs) correspond to the left axis while dairy farms (DFs)

6 correspond to the right axis. Note the DFs are few in some cities and non-existent in

7 some other cities. The number of KFCs in Shaoxing City and Nantong City and the

8 number of ZTOs in Jiaxing City are too few to be simulated. For the real-world data, see

9 [SI Appendix, Fig. S1.](#)